ACS EARTH AND SPACE CHEMISTRY

http://pubs.acs.org/journal/aesccq

Article

Photoreduction of Nitrate to HONO and NO_x by Organic Matter in the Presence of Iron and Aluminum

Published as part of ACS Earth and Space Chemistry special issue "Hartmut Herrmann Festschrift".

Elizabeth Melssen, David L. Bish, Yaroslav Losovyj, and Jonathan D. Raff*

Cite This: *ACS Earth Space Chem.* 2024, 8, 2587−2598

Read Online

ACCESS | Metrics & More | Article Recommendations | Supporting Information

ABSTRACT: Nitrogen oxides (NO_y) such as NO, NO_2, and HONO control the oxidative capacity of the lower atmosphere. Studies have shown that photolysis of nitrate on atmospheric surfaces is an efficient source of nitrogen oxides through a process termed "renoxification;" however, the mechanisms responsible for this process remain poorly understood, leading to difficulties in modeling atmospheric composition. This work aims to elucidate the mechanism of NO_y formation from nitrate photolysis on model boundary layer surfaces comprised of mixtures of organic matter (citrate and Suwanee River fulvic acid) and environmentally relevant metals (e.g., Al^{3+} and Fe^{3+}). Results show that in the presence of organic matter, photochemical yields of NO_y were enhanced by a factor of between 5 and 15 compared with photolysis of pure nitrate controls. Known nitrate photochemistry mechanisms are unable to explain this enhancement, suggesting that a fraction of nitrate is directly converted to NO_y by strong reductants produced photochemically from organic matter. The addition of Fe (hydr)oxides catalyzed both the reduction of NO_2 to HONO and further reduction of HONO to NO via Fe^{2+}, which is formed through photoreduction of Fe-organic matter coordination complexes. In addition, this study assesses the contribution of surface acidity and visible light attenuation on the product yields. The results support a growing body of evidence that strong reductants generated photochemically via organic matter are an important and unrecognized pathway for renoxification on both soil and airborne surfaces (e.g., mineral dust and aerosols).

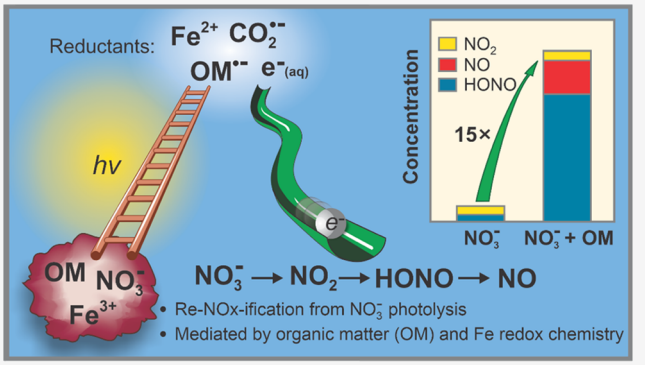

KEYWORDS: *nitrate, photochemistry, nitrous acid, nitrogen oxides, metal oxides, organic matter*

1. INTRODUCTION

Atmospheric composition is significantly impacted by reactive nitrogen oxides (NO_x = NO + NO_2), which control oxidant levels and the photooxidation reaction pathways that remove volatile organic compounds and produce aerosols.[1] However, uncertainty in the sources and sinks of NO_x makes it difficult to accurately predict photochemical air pollution events and assess impacts on climate forcing.[2] One source of NO_x to the troposphere is through the photolysis of nitrate (NO_3^-) adsorbed to boundary layer surfaces (e.g., soil and aerosols).[3−6] Particulate nitrate stems from the hydrolysis of N_2O_5 and OH oxidation of NO_2 to nitric acid (HNO_3) with subsequent gas-to-particle partitioning. Wet and dry deposition is a source of NO_3^- to terrestrial and aquatic systems.[1] Sequestration of NO_x as NO_3^- is temporary, and subsequent photolysis of NO_3^- can release NO_2 and nitrous acid (HONO) in a process termed "renoxification" (R1 and R2).[7−11] Nitrous acid formed in R2 contributes to renoxification by rapidly photolyzing to NO (and OH).[3,7,12]

The quantum yields for reactions R1 and R2 at 298 K at wavelengths above 300 nm are 1.7 and 1%, respectively.[13−15]

$$NO_3^- + h\nu + H_3O^+ \rightarrow NO_2 + OH + H_2O \quad (R1)$$

$$\rightarrow HONO + O(^3P) + H_2O \quad (R2)$$

Numerous studies have found it necessary to consider renoxification via NO_3^- photochemistry to achieve agreement between field observations and models.[16−20] However, the importance of this pathway is debated. Some studies suggest that photolysis of particle-adsorbed HNO_3 or NO_3^- releases NO_2 and HONO at rates that are 300−1000 times faster than expected for the photolysis of aqueous NO_3^- or gas-phase

Received: September 3, 2024
Revised: October 28, 2024
Accepted: November 1, 2024
Published: November 15, 2024

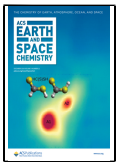

https://doi.org/10.1021/acsearthspacechem.4c00252
ACS Earth Space Chem. 2024, 8, 2587−2598

HNO_3;[18,21−23] other studies suggest the photolysis rate is enhanced by no more than 4 to 10 times.[24,25] The source of this variability is unknown, in part, because photochemical mechanisms of NO_3^- adsorption to boundary layer and aerosol surfaces remain unclear.

Laboratory and field studies point to two possible effects that enhance NO_3^- photolysis rates: (1) Enhancement of the photophysical properties (e.g., quantum yields or absorption cross sections) of surface-adsorbed HNO_3/NO_3^-; and (2) matrix effects involving indirect photochemistry on mineral and/or organic-containing surfaces. Regarding the first possibility, there is evidence that the UV−visible absorption cross sections of HNO_3/NO_3^- may be enhanced by up to a factor of 1000 relative to gas phase HNO_3 at the air−water interface.[13,16,26,27] In addition, HNO_3/NO_3^- adsorbed at the air−water interface may have higher product quantum yields due to an incomplete solvent cage, which could make photoproduct recombination less efficient.[28−30]

The second effect is based on observations that certain particle-phase organic molecules or minerals influence the rate of HNO_3/NO_3^- photolysis and the photoproduct yields.[31,32] For example, studies show that HNO_3/NO_3^- photolysis rates are enhanced when coadsorbed with organic molecules, with the major product being HONO.[5,33] Furthermore, HNO_3/NO_3^- photochemistry may depend on the type of organic matter present, with aliphatic matter being just as important in some cases as chromophoric dissolved organic matter in impacting photoproduct yields from nitrate photolysis.[34−37] Finally, there is evidence that Fe-bearing minerals may play a role in renoxification. For example, field studies have documented increased HONO levels during dust storms,[38,39] and the literature is replete with evidence that reduced iron species present in minerals and in soils can reduce nitrate and NO_2 to HONO and other oxides of nitrogen.[40,41] Unfortunately, most laboratory mechanistic studies to date have been focused on the influence of organic components or salts on renoxification. However, there is still considerable uncertainty about whether renoxification of nitrate is affected by complex matrices that are more representative of soil and mineral dust aerosols.

Soil and mineral dust aerosols contain complex mixtures of organic matter and transition metals and/or redox-active minerals. In addition, aqueous aerosols are known to contain dissolved redox active metals such as Fe^{3+} or Cu^{2+}, which are complexed to organic ligands such as carboxylates or phenolates.[42−44] Metal complexes participate in catalytic redox cycles involving oxygen to generate reactive oxygen species (e.g., Fenton chemistry) that may have a significant effect on oxidation chemistry occurring on the surface or within the particle environment.[45,46] This chemistry can be promoted photochemically as many transition metal complexes strongly absorb UV−visible light via ligand-to-metal charge transfer electronic transitions.[47] Unfortunately, little is known about how interactions between organic matter and transition metals impact renoxification processes on environmentally relevant surfaces.

Here we systematically explore how organic matter and transition metals present in boundary layer surfaces control renoxification from nitrate photolysis through redox chemistry and by influencing the surface pH and light adsorbing properties of the matrix. Using photochemistry experiments in a coated-wall photochemical flow reactor coupled to a sensitive chemiluminescence analyzer designed to measure emitted gaseous NO, NO_2, and HONO, we studied the effect that substrate composition has on the product distribution stemming from photolysis of adsorbed NO_3^-. Substrates consisted of kaolinite, coatings of organic matter proxies (Suwanee River fulvic acid or citric acid), and various amounts of Fe^{3+} and Al^{3+}, that were used to vary the surface pH, redox properties, and light absorption properties of the substrate. Our findings suggest that organic matter and the types of minerals present are important variables driving renoxification from boundary layer surfaces that should be considered when interpreting field data.

2. EXPERIMENTAL SECTION

2.1. Flow Reactor Experiments. Photochemical studies were carried out using a jacketed (25.0 °C) horizontal flow reactor [100 cm long × 2 cm ID].[41,48] The flow reactor was attached to a custom-built single channel chemiluminescence NO_y analyzer (Air Quality Design, Inc.) equipped with a custom-built Nafion converter for quantification of NO, NO_2, and HONO.[49] Detailed descriptions of the converter and measurement cycle are included in the Supporting Information (SI) (Figure S1). During experiments, coated tubes were positioned in the reactor under a flow of carrier gas [1.9 L/min of pure air or N_2 at a relative humidity (RH) of 50%]. RH was set by adjusting the flow of dry and humidified (water trough) ultrahigh purity air or nitrogen, as monitored by a humidity probe (Vaisala, HMT 130). Each sample was given 15 min to equilibrate to establish a background signal in the absence of light. Subsequently, the sample was irradiated with the filtered output (λ > 280 nm) of a 200 W Xe(Hg) arc lamp (Newport) for 1 h. The lamp was positioned so the entire 6.5 cm length of the sample tube was irradiated evenly. The NO_y analyzer measured NO, NO_2, and HONO concentrations in 5 min intervals.[49] Teflon tubing and fittings were used and a perfluorinated polymer (Fluoropel PFC 801A, Cytonix Corp.) coated all exposed metal and glass surfaces to prevent secondary chemistry and wall losses of reaction products.

2.2. Substrate and Coating Procedure. For each experiment, the inner surface of a Pyrex tube (6.5 cm long × 2.22 cm OD) was coated with a thin film of substrate prepared using a method described previously.[41,48] Briefly, kaolinite was combined with either $Fe_2(SO_4)_3$ hydrate or $Al_2(SO_4)_3$ added as a 0−4 wt % addition, where the weight percent (wt %) is calculated from the mass of Fe or Al added relative to the total substrate mass (including the kaolinite and added metals). To this, sodium citrate dihydrate or Suwannee River fulvic acid standard II (SRFA) were added (0 or 2 wt %) and hydrated in a substrate-to-water ratio of 1:1 (w/w) and dried at 40 °C overnight. Hydrolysis of added $Fe_2(SO_4)_3$ and $Al_2(SO_4)_3$ coats kaolinite with a layer of metal hydr(oxy)oxide, which serves as a positively charged adlayer aiding in organic matter adsorption. This layer also promotes protonation of any nitrite formed allowing it to be quantified as $HONO_{(g)}$.[48] The substrate was rehydrated by adding 1 g of water and 1 g of 0.25 M $NaNO_3$ per gram of substrate, resulting in a 2:1 (w/w) liquid-to-solid ratio. The pH was measured using a Mettler Toledo F-20-Kit FiveEasy Benchtop pH meter and adjusted to pH 5.0 ± 0.1 using 1 M NaOH, and 1 M H_2SO_4. This pH was chosen to mimic the pH of a wide range of global soils.[50] Coated tubes were dried at 40 °C and stored in a storage chamber under a flow of air (1.9 L/min at 50% RH) overnight until the experiment was conducted. The resulting coatings

https://doi.org/10.1021/acsearthspacechem.4c00252
ACS Earth Space Chem. 2024, 8, 2587−2598

were uniform in thickness and surface roughness and had a dry mass of 0.30 ± 0.05 g.

2.3. Fe^{2+} Quantification. The amount of Fe^{2+} present in samples following photochemical experiments was determined using the phenanthroline method.[40] This was done by rinsing the coatings on the Pyrex tubes with 10 mL of water. The solid suspension was centrifuged once for 30 min to extract and separate the solid phase and was then syringe filtered (0.2 μm cutoff) to eliminate residual solids. 1,10-phenanthroline monohydrate (phen) was added to the filtrate in stoichiometric excess relative to the amount of iron. The solution was vigorously mixed in the dark for 1 h prior to quantification. Complexed $[Fe(phen)_3]^{2+}$ was transferred to a fused silica cuvette (10 mm path length) and its absorbance was measured at 510 nm via UV−visible spectroscopy (USB4000, Ocean Optics). The absorbance was calibrated from plots of absorbance vs concentration of known amounts of Fe^{2+} derived from the complexation of $FeCl_2{\cdot}6H_2O$ (Sigma-Aldrich) with phen and a 1 mol % solution of 1,4-dihydroxybenzene that was adjusted to pH 3 using solutions of 1 M NaOH and 1 M H_2SO_4.

2.4. Gas-Phase Uptake Experiments. Flow reactor experiments were carried out to study the reactive uptake of $NO_{2(g)}$ and $HONO_{(g)}$ onto the kaolinite substrates containing Fe^{3+}, in the presence and absence of citrate, and prepared according to the procedure described above. Experiments were similar to those described previously.[41,48] Briefly, a constant flow of $HONO_{(g)}$ or $NO_{2(g)}$ was introduced to the flow reactor through a movable injector. This flow was diluted in high purity zero air at 50% RH to achieve a total flow of 1.9 L/min. The experiment was initiated with the injector in a position downstream of the sample to prevent reaction with the substrate and to establish background concentrations of the reactants over the course of 15 min.[49] With the injector still in the downstream position, the shutter to the 200 W Xe(Hg) arc lamp (Newport) (λ > 300 nm) (see spectra in SI Figure S3) was opened, allowing the substrate to be irradiated for 15 min. The injector was then pulled upstream of the sample to expose the substrate to a stream of either 6 ppb $HONO_{(g)}$ or 20 ppb $NO_{2(g)}$ for another 15 min.

2.5. Surface Characterization. Surfaces were characterized by X-ray powder diffraction (XRD) (Figure S2 and Table S1), X-ray photoelectron spectroscopy (XPS) (Table S2), and diffuse reflectance UV−visible spectroscopy (Figure S3). Details of surface characterization are provided in the SI.

3. RESULTS AND DISCUSSION

We conducted a systematic study of the most important variables controlling the photoproducts formed when NO_3^- is photolyzed on complex environmental surfaces. The impact of organic matter (OM) on HONO, NO_2, and NO formation was studied using citrate and Suwannee River fulvic acid (SRFA) as model OM systems. Citrate was chosen as a model for OM because it was previously shown to represent a common type of chelating ligand found in natural organic matter.[51] SRFA was chosen as an organic matter standard because of its well-characterized chemical and physical properties and water solubility.[52] We also compare the photochemistry of NO_3^- in the presence of either Al^{3+} or Fe^{3+} (hydr)oxides. Iron is the most abundant redox-active metal and a major component of aerosol, dust particles, and soil surfaces[39,42,53,54] and it has been shown that Fe^{2+} present in minerals or generated[55−57] photochemically can reduce NO_2 to HONO.[40] Furthermore, Fe^{3+} complexes involving carboxylic acids such as citric acid or those present in NOM possess strong ligand-to-metal charge transfer absorption bands making them potentially important environmental chromophores.[58] Thus, comparing NO_3^- photochemistry in the presence of Fe^{3+} (hydr)oxides with what happens in the presence of redox-inactive Al^{3+} highlights the role of transition metals on surface NO_y chemistry. Finally, we consider the effect of surface pH, light attenuation, and secondary reactions involving the reactions of primary photoproducts and redox-active organic and inorganic species on the surface. Together, the observations are used to propose a mechanism for the observed photoproduct enhancements.

3.1. Effect of Organic Matter on Nitrate Photoproduct Formation. Nitrate adsorbed to substrates consisting of kaolinite with 2 wt % aluminum sulfate (Al^{3+}) was irradiated (λ > 280 nm) in the absence or presence of citrate or SRFA in 1 atm of air at an RH of 50% ± 3. In the absence of organic matter, NO_3^- photolysis generates NO_2 as the main product with small amounts of HONO (Figure 1A; 0−75 min), consistent with reactions R1 and R2. When the experiment is repeated in the presence of sodium citrate (Figure 1A; 80−160 min), the main photoproduct is HONO, with lesser amounts of NO_2 and NO generated. Notably, the amount of HONO formed is not stable, rising sharply when the substrate is exposed to light, but decaying exponentially over the course of the experiment. When the experiment is repeated by replacing citrate with SRFA, (Figure 1A; 175−250

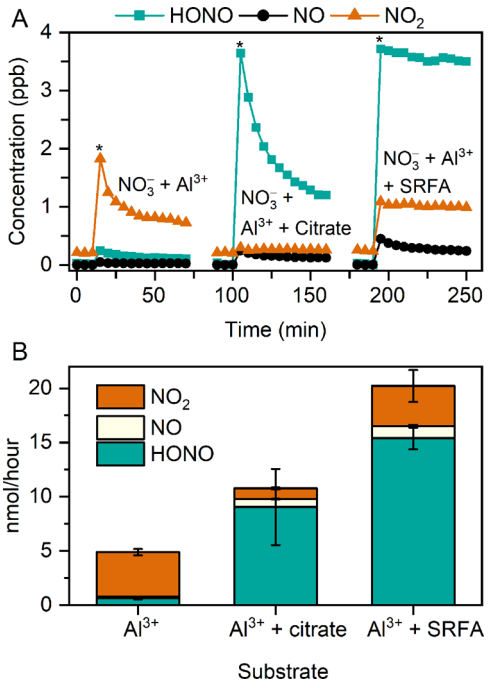

Figure 1. Organic matter [citrate or Suwannee River fulvic acid (SRFA)] enhances the amount of NO_x and HONO formed during NO_3^- photolysis on surfaces comprised of Al^{3+} [added as $Al_2(SO_4)_3$] and kaolinite (substrate pH: 5; carrier gas: 1 atm air, 50% RH). (A) Kinetic traces of photoproducts formed from photochemistry of the indicated substrates, where asterisks represent the beginning of a 60 min irradiation with UV−visible light. (B) Total amount of indicated photoproducts formed over the course of the experiment, derived by integrating the data in panel (A). Error bars are 95% confidence intervals of triplicate experiments.

https://doi.org/10.1021/acsearthspacechem.4c00252
ACS Earth Space Chem. 2024, 8, 2587−2598

min) a large amount of HONO is generated along with measurable amounts of NO_2 and NO. In contrast to the experiment involving citrate, the amounts of HONO and NO_x formed are stable over the 60 min irradiation period in the presence of SRFA. The difference between these two experiments suggests that citrate is unable to sustain the photochemistry at initial levels, possibly indicating that reactive moieties (e.g., radical byproducts) are consumed during the reaction. This is consistent with the work of Zhang et al., who showed that photodegradation of Fe^{3+}-citrate leads to fragmentation of ligand to alkyl radicals and stable ketone/aldehyde photoproducts, which would lead to loss of Fe^{3+}-citrate complexes in their system.[59] In the case of SRFA, light appears to sustain the chemistry, suggesting that reactive moieties involved in product formation are regenerated upon irradiation. As shown previously, quinone moieties present in NOM are photoreduced to hydroquinones,[41] which are strong reducing agents known to promote redox chemistry.[60]

To facilitate comparisons, we report product formation rates (in nmol h^{-1}) as quantified by integrating the respective concentration vs time profiles shown in Figure 1A. As shown in Figure 1B, eight times more HONO and three times less NO_2 are generated when NO_3^- is photolyzed in the presence of citrate than were observed in the absence of OM. In the presence of SRFA, HONO production is enhanced by more than a factor of 15 relative to when NO_3^- is photolyzed in the absence of OM. In the presence of OM, HONO amounted to between 70−75% of the total NO_y detected, whereas in the absence of OM, HONO accounted for 20% of total NO_y. Nitric oxide (NO) is only detected in the presence of either citrate or SRFA, but not in the absence of OM.

3.2. Effect of Transition Metals on Nitrate Photolysis Product Yields. We next explored the impact of Al^{3+} and Fe^{3+} on NO_3^- photochemistry. The amount of Al^{3+} or Fe^{3+} present in the substrate was varied between 0−4 wt % (relative to kaolinite) in the presence and absence of citrate or SRFA to evaluate the effect of transition metals on the rate of nitrate photoproduct formation. In these experiments, the amount of OM used was held constant at 2 wt % relative to kaolinite, as this resulted in the most reproducible data. Figures 2A and 3A show how formation rates of HONO and NO_x vary with the Al^{3+} or Fe^{3+} content of the substrate, respectively; the relative amount of each photoproduct formed for each experiment is shown in Figures 2B and 3B.

As shown in Figure 2A, the amount of HONO produced when NO_3^- was photolyzed in the absence of OM decreased slightly as the amount of Al^{3+} added to the kaolinite substrate was increased from 0 to 4 wt %; the amount of NO_2 formed was relatively insensitive to the presence of Al^{3+}, although a slower formation rate occurred at 4 wt %. In contrast, the amount of HONO formed from NO_3^- photolysis in the presence of citrate increased by a factor of 6 as the amount of Al^{3+} was increased from 0 to 4 wt %. A similar effect was observed when Al^{3+} was added to substrates containing SRFA, although in this case, a factor of 2 enhancement was observed. The amount of NO_2 formed increased as Al^{3+} content increased for the SRFA system; however, as shown in Figure 2B HONO was the main product (between 80−90%) formed in the presence of OM.

Replacing Al^{3+} with Fe^{3+} resulted in notable differences in the amount of HONO and NO_x formed during NO_3^- photolysis. As shown in Figure 3A, the amount of HONO and NO_2 formed was reduced by half when NO_3^- was

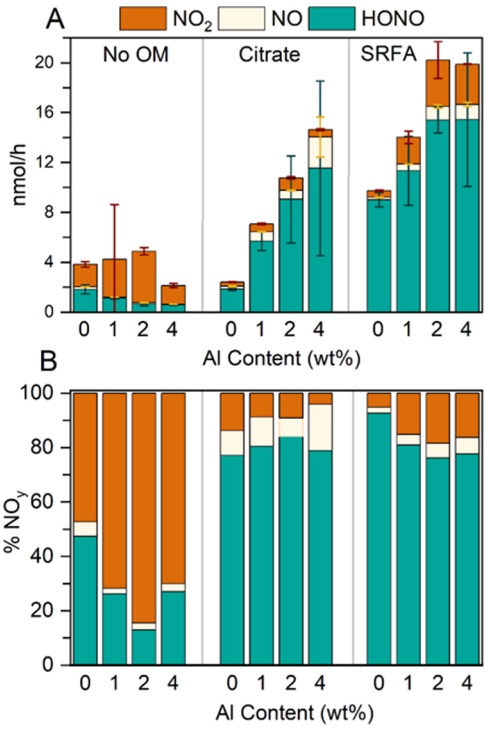

Figure 2. (A) Comparison of amount of NO_x and HONO formed during 1 h of UV−visible photolysis of NO_3^- on kaolinite substrates containing various amounts of Al^{3+} [added as $Al_2(SO_4)_3$] in the absence or presence of 2% OM citrate or Suwanee River fulvic acid (SRFA) (substrate pH: 5; carrier gas: 1 atm air, 50% RH). Error bars represent 95% confidence intervals of triplicate experiments. (B) Relative amounts of photoproducts formed from experiments are shown in panel (A).

photolyzed in the presence of Fe^{3+} (no added OM). In the presence of OM, the total amount of NO_y increased between 0−2 w% Fe^{3+} but a drop in reactivity was seen at the 4 wt % Fe^{3+} level. In the case of citrate, the main photoproducts were HONO and NO, with minor amounts of NO_2 formed (Figure 3B). In the case of SRFA, HONO was the main product, although in the presence of Fe^{3+} up to 10% of the NO_y formed was NO.

3.3. Differences between Iron and Aluminum. In general, photolysis of NO_3^- in the presence of Al^{3+} produced higher amounts of NO_y compared with Fe^{3+}, with HONO being the dominant photoproduct in the presence of OM. This is especially noticeable when NO_3^- was photolyzed on Al^{3+}-citrate coated substrates, which produce 2−3 times more NO_y than the analogous Fe^{3+} system. Likewise, the Al^{3+}-SRFA systems produced 1.3 times more NO_y than their Fe^{3+} counterparts. The following may explain this difference in behavior: (1) Disparate light absorption and attenuation characteristics; and (2) Fe^{3+} and Al^{3+}-coated substrates differ in surface acidity, which impacts the amount of HONO released from the surface. Below, we examine each of these possibilities to provide a basis for assessing the influence of Fe^{3+} and Al^{3+} on the amount of NO_3^- photoproducts formed.

3.3.1. Substrate Light Absorption and Attenuation. For insights into the light absorbing properties of the substrates, samples were analyzed by diffuse reflection UV−visible absorption spectroscopy. We found that kaolinite and kaolinite coated with Al (hydr)oxides and/or citrate absorbed weakly at wavelengths above 300 nm, which is the lamp cutoff through

https://doi.org/10.1021/acsearthspacechem.4c00252
ACS Earth Space Chem. 2024, 8, 2587−2598

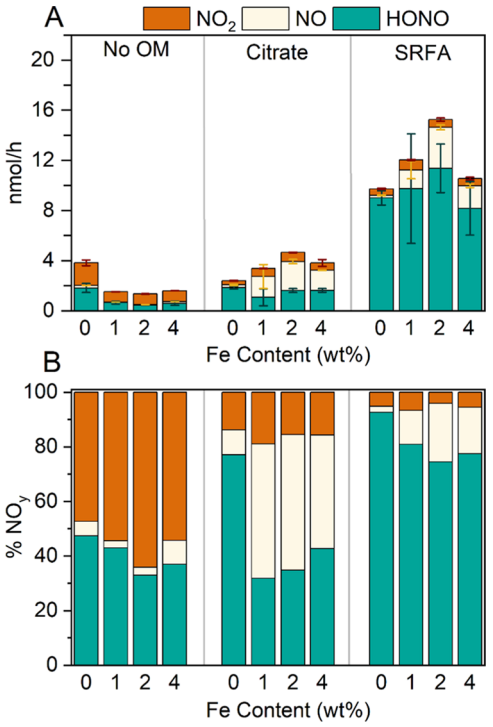

Figure 3. (A) Comparison of amount of NO_x and HONO formed during 1 h of UV−visible photolysis of NO_3^- on kaolinite substrates containing various amounts of Fe^{3+} [added as $Fe_2(SO_4)_3$] in the absence or presence of 2% OM citrate or Suwanee River fulvic acid (SRFA) (substrate pH: 5; carrier gas: 1 atm air, 50% RH). Error bars represent 95% confidence intervals of triplicate experiments. (B) Relative amounts of photoproducts formed from experiments are shown in panel (A).

glass (Figure S3B). This suggests the substrates are relatively transparent to incident light from the photolysis lamp. Significantly higher light absorption was observed for substrates containing iron, including Fe-containing samples with added citrate and SRFA (Figure S3A). Addition of Fe^{3+} caused substrates to absorb out to ∼600 nm and beyond when SRFA was present, which has significant implications for understanding the photochemistry observed in Figures 1−3. First, it suggests that Fe-containing substrates are photoactive over a wide range of the actinic spectrum. This includes the ability of Fe^{3+} to undergo photoreduction to Fe^{2+}, which is a strong reducing agent and could participate in secondary chemistry involving NO_y. Second, strong UV−visible absorbance by iron-containing substrates screens light transmission through the sample. Nitrate salts absorb at wavelengths less than ∼320 nm (Figure S4); thus, strong light absorption by coadsorbed Fe^{3+} (hydr)oxides could effectively retard the rate of NO_3^- photolysis.

3.3.2. Surface Acidity Effects on HONO Volatilization. Surface acidity is hypothesized to play a role in controlling redox conditions and determining the amount of adsorbed NO_2^-NO that is volatilized from the substrate surface. Previous studies have shown that metal (hydr)oxide surfaces are comprised of $M-OH_2^+$ groups (where M = Al^{3+} or Fe^{2+}) over a wide pH range that acidify the thin water layers coating mineral surfaces.[48] In the case of Al^{3+} (hydr)oxides such as gibbsite, it is thought that the relevant reactive sites are aluminol groups occurring at steps and edges of the exposed aluminum oxide layers that have pK_a values of ∼6.5.[61,62] Coating of the kaolinite substrate with Al^{3+} (hydr)oxides creates an abundance of $Al-OH_2^+$ sites that we showed previously promote the protonation of $NO_2^-{}_{(aq)}$ to HONO.[41,48] Similar surface acidity is thought to occur on Fe (hydr)oxide surfaces. To test this assumption, we titrated kaolinite substrates coated in either Al^{3+} or Fe^{3+} (hydr)oxide with 1 nmol of $NaNO_{2(aq)}$ and monitored the formation of $HONO_{(g)}$. In both cases, addition of $NO_2^-{}_{(aq)}$ to the substrate resulted in a pulse of $HONO_{(g)}$ (Figure S5). Peak areas indicate twice as much $HONO_{(g)}$ was produced on Al^{3+} (hydr)oxides surfaces compared with Fe^{3+} (hydr)oxide surfaces, indicating that surfaces comprised of Al^{3+} were more acidic. As the concentration of the metal increases, surface acidity also increases, facilitating the increase of gas-phase products observed. This suggests that the higher yields of HONO observed in Al vs Fe-coated surfaces in Figures 2 and 3 are due at least partially to a surface pH effect. In summary, both surface pH and light attenuation act together leading to 25−50% more NO_y formed from the Al^{3+} systems compared with the Fe^{3+} systems.

3.4. Origin of Nitric Oxide. Although NO is not produced by the direct photolysis of NO_3^-, it is formed from photodissociation of NO_2 and HONO. Control experiments showed, however, that photolysis of NO_2 and HONO was minimal; the relative amount of NO formed from direct photolysis of these species (1−5%) is reflected in the experiments labeled "No OM" in Figures 2 and 3. The addition of Fe^{3+} to substrates containing OM dramatically increased the amount of NO formed (Figure 3). For example, when NO_3^- was photolyzed on substrates containing both Fe and citrate, NO accounted for ∼50% of the NO_y formed. Similarly, up to 20% of the NO_y detected was in the form of NO for substrates prepared from SRFA and Fe^{3+}. This suggests NO formation is related to the presence of iron complexed to OM, although NO formation (e.g., 5−15% of the total NO_y formed, Figure 2) was also observed in the presence of Al^{3+} and OM, albeit to a lesser degree.

3.4.1. Influence of Anoxic vs Aerobic Conditions on NO Formation. To further investigate the role of iron on NO formation, we compared the amount of NO_y photoproducts formed when NO_3^- was photolyzed on Fe^{3+} surfaces with citrate or SRFA in the presence and absence of O_2. As shown in Figure 4A,B, photolysis experiments using Fe-containing substrates conducted under N_2 atmosphere produced 2−4 times more NO than experiments conducted under the same conditions but with air as the carrier gas. Under anoxic conditions NO accounted for 60−80% of the total NO_y formed. When these experiments were repeated using Al-containing substrates, we found there was no significant difference between the amount of NO formed under anoxic or oxic conditions (Figure 4A,B). Differences in the response of Fe and Al-containing systems toward O_2 strongly suggest that ferrous iron (Fe^{2+}) is responsible for the NO formed in the systems containing iron. It is well-known that photolysis of iron complexes such as iron citrate is a source of Fe^{2+}.[47,63] Once formed, Fe^{2+} is capable of reducing NO_2 to HONO, and HONO to NO.[40] The feasibility is illustrated in Table S3, which uses reduction potentials of the respective half-reactions to derive the Gibbs free energy of reactions involving Fe^{2+} with various NO_y species. The calculations suggest that reduction of both NO_2 and HONO by Fe^{2+} citrate is exergonic (−66 and −37 kJ mol^{-1}, respectively) at pH 5. This strongly suggests that iron complexes such as iron citrate are capable of

https://doi.org/10.1021/acsearthspacechem.4c00252
ACS Earth Space Chem. 2024, 8, 2587−2598

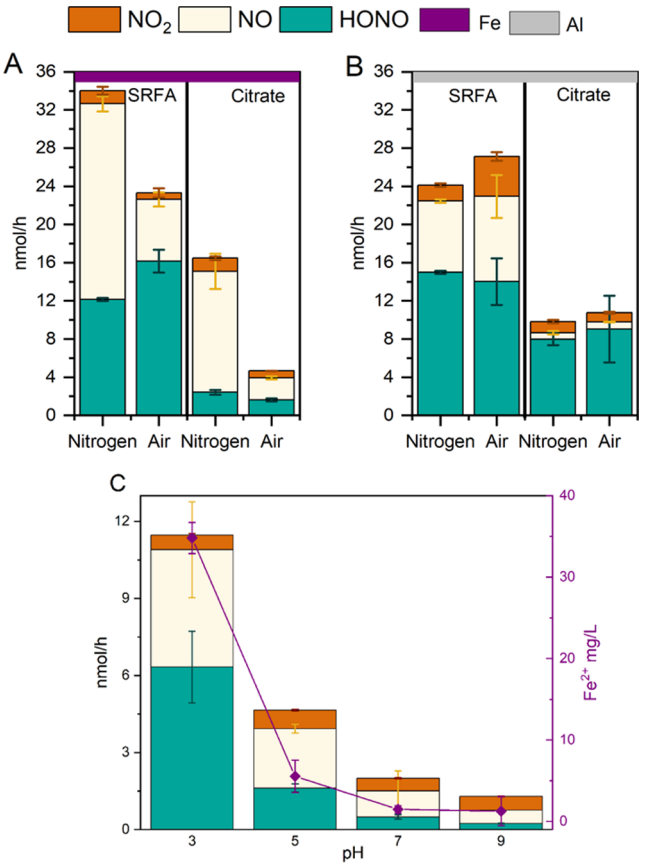

Figure 4. Comparison of NO_x and HONO formed during NO_3^- photolysis in the presence of iron (A) or aluminum (B) and the indicated OM under oxic and anoxic conditions. (C) Bars indicate amount of NO_x and HONO formed when NO_3^- is photolyzed on Fe-containing substrates prepared from aqueous slurries at the indicated pH values. The amounts of Fe^{2+} extracted from substrates post experiment (purple diamonds, right *y*-axis) are shown for comparison. All substrates contained 2 wt % OM (citrate or SRFA) and the metal (Fe^{3+} or Al^{3+}). Error bars represent 95% confidence interval of triplicate measurements.

promoting NO_2-to-HONO and HONO-to-NO formation, which is a potentially important renoxification mechanism.

3.4.2. Influence of pH on NO Formation. For more insight into the role of Fe^{2+} in the photolysis mechanism, we photolyzed NO_3^- on Fe-containing substrates prepared from slurries that had a pH of between 3−9. During these experiments, photoproducts were measured via online CL analysis, whereas Fe^{2+} formed in the substrate was quantified post-experiment using the phenanthroline assay.[40] As shown in Figure 4C, a direct correlation was observed between the amount of photoproducts formed and the amount of Fe^{2+} dissolved in the substrate extracts postexperiment. In addition, the amount of NO formed was highest at the lowest pH values. It is well established that under acidic conditions, iron minerals undergo reductive dissolution to release Fe^{2+}, a process that can be facilitated by photochemistry.[43,53,64,65] This supports the hypothesis that Fe^{2+} plays a role in determining the product distribution by reducing photoproducts. These findings help explain the results in Figure 2A where the relative amount of NO produced increases with increasing iron content of the substrate.

3.4.3. Reactive Uptake of NO_2 and HONO on Fe-Containing Surfaces. As further confirmation of the role that Fe^{2+} plays in secondary chemistry, we studied the reactive uptake of $NO_{2(g)}$ and $HONO_{(g)}$ on iron-coated surfaces in the presence and absence of citrate. NO_3^- was not present during these experiments. Substrates were exposed in the dark to $NO_{2(g)}$ or $HONO_{(g)}$ through the carrier gas (50% RH in air) for ∼15 min, followed by a 15 min period where the substrates were irradiated with UV−visible light. As shown in Figure 5A,

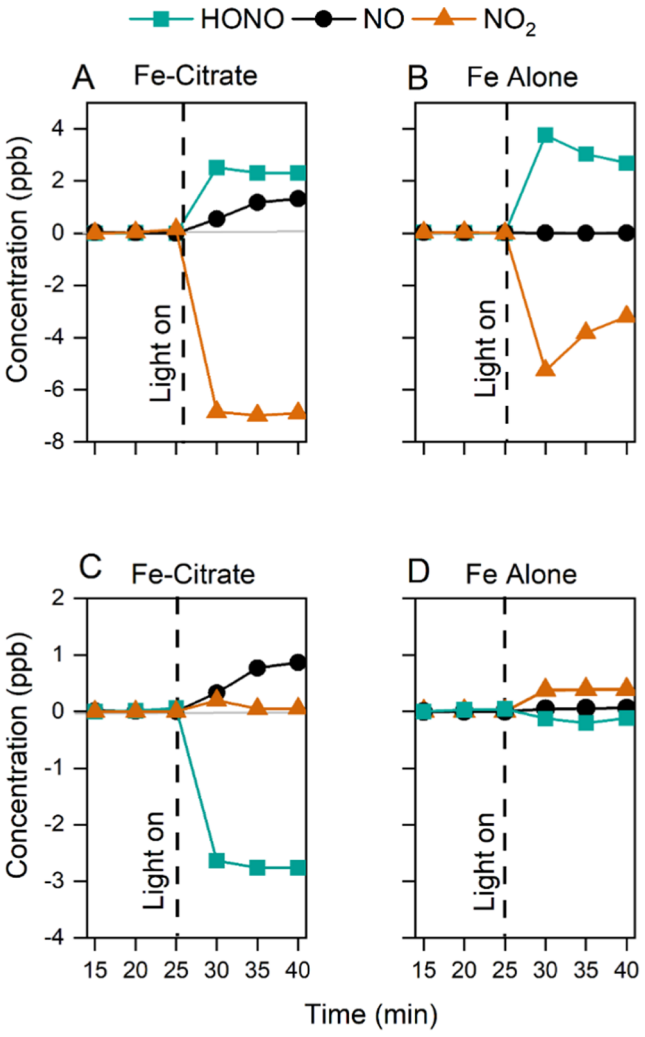

Figure 5. Photoinduced reactive uptake of NO_2 (A, B) or HONO (C, D) on kaolinite surfaces containing 2 wt % Fe^{3+} in the presence or absence of 2 wt % citrate. Samples were exposed to 6 ppb of HONO or 20 ppb of NO_2 in the dark for the first 15 min and then irradiated for the 15 min with UV−visible light as indicated by the vertical dashed line. Carrier gas: 1 atm air at 50% RH; substrate pH: 5.

exposure of Fe-citrate-coated substrates to 20 ppb of NO_2 in the dark did not yield any HONO or NO; however, when irradiated with UV−visible light, 7 ppb of NO_2 was lost to the surface and 2.5 ppb of HONO and 1.5 ppb of NO were formed. This demonstrates that NO_2 is reduced to HONO and NO during the reaction. The appearance of NO is more gradual than the appearance of HONO, suggesting that NO is a secondary product. HONO was the only product observed when NO_2 was photolyzed in the presence of kaolinite coated with Fe (hydr)oxides (Figure 5B). In this case, 5.5 ppb of NO_2 was initially taken up although this decreased to ∼3 ppb by the end of the experiment, suggesting that the reactive sites were

https://doi.org/10.1021/acsearthspacechem.4c00252
ACS Earth Space Chem. 2024, 8, 2587−2598

A

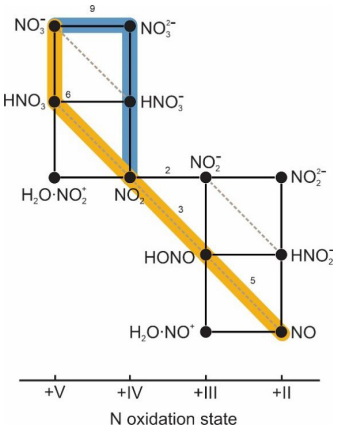

B

#	Reduction half reaction	$E°$ (V) vs SHE, pH 5
1	$^3DOM^* + e^- \rightarrow DOM^{*-}$	1.58
2	$NO_2 + e^- \rightarrow NO_2^-$	1.07
3	$NO_2 + H^+ + e^- \rightarrow HONO$	0.77
4	$Fe^{3+}(aq) + e^- \rightarrow Fe^{2+}(aq)$	0.77
5	$HONO + H^+ + e^- \rightarrow NO + H_2O$	0.69
6	$NO_3^- + 2H^+ + e^- \rightarrow NO_2 + H_2O$	0.50
7	Fe^{3+} citrate $+ e^- \rightarrow Fe^{2+}$ citrate	0.37
8	$SRFA + e^- \rightarrow SRFA^{\bullet-}$	−0.49
9	$NO_3^- + e^- \rightarrow NO_3^{2-}$	−0.89
10	$CO_2 + e^- \rightarrow CO_2^{\bullet-}$	−1.95

Figure 6. (A) Scheme of squares depicting redox pathways involved in reduction of NO_3^-. Lines between chemical species represent the following equilibrium reactions: Electron transfer (horizontal lines), proton transfer (vertical lines), and diagonal dashed lines (coupled proton−electron transfer). Yellow highlighted pathway indicates the proposed NO_3^- photoreduction mechanism under acidic conditions with NO_3^- reduction by Fe^{2+} citrate and $SRFA^{\bullet-}$. Blue highlighted pathway indicates pathways available when $CO_2^{\bullet-}$ or solvated electrons are the reductant. Numbers over lines correspond to the half reactions listed in panel (B) Selected half reactions for relevant processes in the system and their reduction potential for pH 5.

depleted over the course of the reaction. The amount of HONO formed from NO_2-to-HONO conversion varied between 3−4 ppb. This result contrasts with those from the experiment performed in the presence of citrate, which showed relatively constant NO_2-to-HONO conversion during the irradiation period. These results suggest that photolysis of iron in the presence of citrate generates a relatively constant source of Fe^{2+}. In addition, the appearance of NO as a product in the presence of citrate (and not when Fe is present alone) suggests that stronger reducing agents are likely formed in the presence of citrate.

Previous studies indicate that Fe^{2+} present in iron-bearing minerals reduces NO_2^- to NO, in some cases contributing to abiotic emissions of NO from soil.[66] To determine whether the NO observed in Figure 5A stems from the reduction of NO_2^-/HONO by Fe^{2+}, we studied the photochemical uptake of $HONO_{(g)}$ onto iron-containing kaolinite substrates in the presence and absence of citrate. The experiments performed were identical to those shown in Figure 5A,B with the exception that the carrier gas contained 6 ppb of $HONO_{(g)}$. As shown in Figure 5C, exposure of the Fe-citrate coated kaolinite substrate to HONO in the dark did not result in the formation of NO_y; however, during irradiation of the substrate, 2.7 ppb of HONO was lost to the surface yielding the gradual formation of ∼1 ppb of NO. These results resemble the HONO and NO profiles shown in Figure 5A, strongly suggesting that the observed NO stems from the reduction of NO_2^-/HONO to NO. These results contrast with those obtained when the experiment was repeated in the absence of citrate. As shown in Figure 5D, in the absence of citrate, HONO uptake on the surface when the surface is irradiated with UV−visible light was much lower than what was observed in the presence of citrate. These results suggest that iron coordinated to citrate is responsible for the reduction of NO_2^-/HONO to NO. This is a reasonable assumption since the stability constants for $Fe^{3+}(citrate)_{(aq)}$ and $Fe^{2+}(H\text{-}citrate)_{(aq)}$ complexes are large ($\log K$ = 13.13 and 10.17, respectively).[67] Considering the reduction potentials of the relevant half reactions at pH 5 (see Figure 6 and Table S3), we find that HONO-to-NO conversion by Fe^{2+}-citrate is exergonic, whereas the reaction of the Fe^{2+} aquo complex with HONO is endergonic, reflecting the fact that ferrous citrate is a stronger reducing agent than the Fe^{2+} aquo ion.[47]

3.5. Proposed Reaction Mechanisms. Significant enhancements in NO_y production rates are evident in the presence of OM versus NO_y produced when nitrate is photolyzed alone, which is the trend seen for both Al- and Fe-containing substrates. As discussed above, it is well documented that OM acts as both a scavenger of OH that prevents the oxidation of photoproducts and generates HO_2/O_2^-, which converts NO_2 and NO into NO_2^-/HONO.[14,34,37,68,69] In addition, OM-containing photosensitizer moieties are known to efficiently reduce NO_2 to NO_2^-/HONO with near quantitative efficiency.[41,69,70] Thus, if the quantum yield of the NO_3^--to-HONO photochemical channel is ∼1% in the absence of OM, then it should increase by a factor of 2 at most if all NO_2 formed is converted into NO_2^-/HONO in the presence of OM. As shown in Figures 1−3, the enhancement in NO_y yield is greater than expected; e.g., the HONO concentration is enhanced by a factor of 15 in the presence of 2 wt % SRFA.

Based on our results, we propose that nitrate is directly reduced to either NO_2 or the nitrate dianion NO_3^{2-} (or its conjugate acid, HNO_3^-, pK_a ∼ 7.5) by a reactive species generated photochemically in the presence of OM.[71] Nitrate dianion has been observed in aquatic radiolysis experiments where it is formed from the reaction of solvated electrons with NO_3^-. Although known since the 1960s in the radiolysis literature,[71−73] the involvement of NO_3^{2-} has only now been considered as an intermediate in the photoreduction of nitrate under atmospheric conditions.[31,74] To provide support for this mechanism and the subsequent reaction steps, we compiled reduction potentials of relevant half-reactions from the literature (Figure 6 and Table S4) and used them to compute the Gibbs free energy of the proposed reaction steps (Table S3). Although comparisons of Gibbs free energy only indicate whether a reaction is thermodynamically feasibility and say nothing of its kinetics, the process is a valuable guide to unveiling previously unrecognized reaction steps of a mechanism.

https://doi.org/10.1021/acsearthspacechem.4c00252
ACS Earth Space Chem. 2024, 8, 2587−2598

To illustrate our proposed mechanism involving redox chemistry, we use a scheme of squares to summarize the conversion of NO_3^- to NO (Figure 6A). In this figure, the redox processes are described as either a decoupled sequence of one-electron transfer (horizontal arrows) and one-proton transfer (vertical arrows) or a coupled proton−electron transfer process (diagonal arrows). Reduction half reactions along with reduction potentials of some of these reactions are listed in Figure 6B. As shown in Figure 6A, NO_3^{2-}/HNO_3^- would rapidly hydrolyze to NO_2, which in turn would be reduced to N(III) species such as NO_2^-, HONO, or H_2ONO^+, depending on the pH. From here, one electron reduction of N(III) yields NO. Under the more acidic conditions of our experiment, HONO is likely reduced to NO via coupled proton−electron-transfer as supported by data in Figure 5, but at higher pH values, reduction of NO_2^- could involve the intermediate NO_2^{2-} and HNO_2^- species via a mechanism that is analogous to the one proposed for hydrolysis of NO_3^{2-}/HNO_3^-, and has been discussed previously in the radiolysis literature.[73]

Strong reducing agents are needed to directly reduce NO_3^- to NO_x and HONO. In systems containing SRFA, reducing agents are generated when the triplet excited state of SRFA reacts with an electron donor to form a radical anion, $SRFA^{\bullet-}$. Likewise, organic coordination complexes of Fe^{2+} formed through photochemistry are strong reductants.[44,47] Given the high negative reduction potential for the NO_3^-/NO_3^{2-} redox couple, $E^\circ = -0.89$ V vs SHE, it appears that Fe^{2+}-citrate and $SRFA^{\bullet-}$ are not likely to reduce NO_3^- via eq 9 (Figure 6B); Gibbs free energy values are highly endergonic (Table S3). There is evidence that nitrate is reduced rapidly to NO_3^{2-} by solvated electrons ($k = 9.7 \times 10^9$ M^{-1} s^{-1})[73] generated via dissociation of water by ionizing radiation. Solvated electrons have been observed to be generated photochemically in dissolved organic matter and it is possible that they could play a role in the chemistry observed here.[75−77]

Alternative reaction pathways exist to convert NO_3^- to NO_2 without involvement of NO_3^{2-}. As shown by their exergonic Gibbs free energy values in Table S3, both $SRFA^{\bullet-}$ and Fe^{2+}-citrate can reduce NO_3^- to NO_2 under acidic conditions, likely via the intermediacy of NO_2^+ (eq 6). The substrates we studied were prepared from aqueous slurries adjusted to pH 5, although it is possible that hydronium and acidic $M-OH_2^+$ groups are concentrated into a much smaller volume defined by a few monolayers of water present on the surfaces.[78,79] Thus, if we assume 1−2 monolayers of water present on a typical kaolinite surface (at 50% RH),[48] the surface acidity could be quite high. This is supported by the titration experiment shown in Figure S5. The reduction potential estimated for eq 6 was calculated for pH 5, and lower surface pH values would only increase the reduction potential, making this reaction even more thermodynamically feasible.

Reducing agents such as Fe^{2+}-citrate and $SRFA^{\bullet-}$ clearly cannot explain the high reactivity present when NO_3^- is photoreduced in the presence of Al^{3+}-citrate, as they are not present in those systems. Furthermore, we are unaware of any literature showing that photochemistry involving Al-citrate could lead to the formation of solvated electrons. To explain the high reactivity of Al^{3+}-citrate, we consider the possibility that carbon dioxide radical anion ($CO_2^{\bullet-}$) or its conjugate acid ($CO_2H^\bullet$, $pK_a = 3.4$) is generated upon irradiation of citrate or aluminum citrate, or through the reaction of citrate with OH radical generated from NO_3^- photolysis.[80]

Numerous studies have shown that $CO_2^{\bullet-}$ is generated during the oxidation of carboxylate anions. Most relevant, $CO_2^{\bullet-}$ was shown to be generated from the reaction of formate with OH radical generated from nitrate.[81] In addition, EPR studies show $CO_2^{\bullet-}$ is generated from photolysis of iron citrate, and aerosol studies show prompt decarboxylation releases CO_2 and HO_x into the gas phase.[82,83] We propose that this could also be the case for the analogous Al^{3+}-complexes. The carbon dioxide radical anion is a strong one-electron reductant that can directly reduce NO_3^- to NO_3^{2-} (Figure 6B and Table S3).[73] Although citrate and Al^{3+}-citrate absorb only weakly at wavelengths greater than 300 nm (Figure S3), $CO_2^{\bullet-}$ is expected to be reactive and the nitrate concentrations are high enough in our system such that even trace amounts of $CO_2^{\bullet-}/CO_2H^\bullet$ could reduce NO_3^-, NO_2, and HONO.[84]

We also note that there is the possibility that $CO_2^{\bullet-}$ is produced from the reaction of Al^{3+} citrate with OH generated from nitrate photolysis. These reactions have not received much attention and work is underway in our laboratory to evaluate their reaction kinetics. Lastly, it is possible that formation of $CO_2^{\bullet-}/CO_2H^\bullet$ occurs during photochemistry in the Fe^{3+}-citrate and SRFA studied here. Photochemistry involving UV−visible absorption by natural OM is known to produce CO_2 and carboxylate species as a result of direct and indirect photochemistry.[85,86] Thus, it is possible that the chemistry observed for simple model carboxylates also occurs in more complex OM mixtures.

5. CONCLUSIONS

This work showed that NO_3^- adsorbed to mineral surfaces undergoes renoxification to release HONO and NO via the reaction of nitrate with strong reducing agents stemming from indirect photochemistry involving transition metal complexes and organic matter. A 15-fold enhancement in NO_y yield was observed when NO_3^- was photolyzed in the presence of OM, relative to when photolysis took place in the absence of OM. Such enhancements are beyond what is expected from the canonical NO_3^- photolysis mechanism and can only be explained by chemistry involving the direct reduction of NO_3^-. Based on thermodynamic considerations of relevant half reactions, candidates for reductants responsible for directly reducing NO_3^- are C-centered radical anions (e.g., $SRFA^{\bullet-}$), Fe^{2+} coordinated to OM, $CO_2^{\bullet-}$, and possibly solvated electrons. Additionally, we showed that renoxification of NO_3^- is not just limited to release of NO_2 and HONO but can also involve formation of NO formed from the reduction of N(III) by strong reducing agents such as those provided by Fe^{2+} complexes. Thus, NO is formed via indirect photochemistry rather than by direct photolysis of NO_2 and HONO. Much of the proposed chemistry is based on precedent in the radiolysis literature and aquatic chemistry community. Future work is needed to directly observe and study the reaction kinetics of these reductants in atmospherically relevant systems. For example, rate constants for the reaction of $CO_2^{\bullet-}$ with nitrate are needed to explicitly describe this chemistry in aqueous aerosol models. In the absence of this information, parameterizations of nitrate renoxification may be based on aqueous phase nitrate photochemistry and by assuming the total product quantum yield for NO_2 and HONO is increased by a factor of between 5−15, based on our work. It is notable that these quantum yield enhancement factors are within the range of 1−30 suggested by Romer et al. for renoxification from aerosol nitrate.[17]

https://doi.org/10.1021/acsearthspacechem.4c00252
ACS Earth Space Chem. 2024, 8, 2587−2598

Even though this study used model soil and mineral dust systems, the components used, and their properties mimic natural systems; thus, we expect similar processes to occur in mineral dust aerosols and on soil surfaces exposed to sunlight. Redox-active transition metals and OM are commonly colocated in mineral dust aerosols from a variety of anthropogenic and biogenic sources.[54,87] These aerosols undergo long-range transport[39] and mix with polluted air masses, where they become acidified as they accumulate nitric and sulfuric acid.[88,89] Our work suggests that photochemistry on dust particles could initiate renoxification episodes during dust storms. Such events were documented by Wang et al. during their field campaign in Phoenix, AZ, in 2001.[38] During that study, the concentration ratio of $HONO/NO_2$ increased from <0.03 during a clear day, to 0.19 during dust storms. Since their study, high $HONO/NO_x$ ratios have been found to be correlated to other air pollution events involving high particulate matter levels.[9,90,91] In addition, recent modeling studies showed that photocatalytic conversion of nitrate on iron-containing mineral dust could be the main source of HONO (up to 62%) during the daytime in the remote marine atmosphere at Cape Verde.[92] In summary, direct reduction of NO_3^- appears to be an efficient renoxification mechanism that may help explain some of the missing daytime sources of HONO inferred from models.[93,94] This source should be implemented into current atmospheric models to better understand the oxidative capacity of the atmosphere.

■ ASSOCIATED CONTENT

Supporting Information

The Supporting Information is available free of charge at https://pubs.acs.org/doi/10.1021/acsearthspacechem.4c00252.

Additional experimental details include: chemicals; details of NOy measurements; surface characterization using X-ray powder diffraction, X-ray photoelectron spectroscopy, and UV-visible spectroscopy; supporting experiments investigating surface acidity; and Gibbs free energy calculations (PDF)

■ AUTHOR INFORMATION

Corresponding Author

Jonathan D. Raff − *Department of Chemistry, Indiana University, Bloomington, Indiana 47405, United States; Paul H. O'Neill School of Public and Environmental Affairs, Bloomington, Indiana 47405, United States;* orcid.org/0000-0002-2574-8061; Email: jdraff@iu.edu

Authors

Elizabeth Melssen − *Department of Chemistry, Indiana University, Bloomington, Indiana 47405, United States*

David L. Bish − *Department of Chemistry, Indiana University, Bloomington, Indiana 47405, United States*

Yaroslav Losovyj − *Department of Chemistry, Indiana University, Bloomington, Indiana 47405, United States*

Complete contact information is available at: https://pubs.acs.org/10.1021/acsearthspacechem.4c00252

Funding

This work was supported by a grant from the U.S. National Science Foundation (NSF) (CHE-2305078). E.M. was partially supported by an Indiana Space Grant Consortium Graduate Student Fellowship.

Notes

The authors declare no competing financial interest.

■ ACKNOWLEDGMENTS

This paper is dedicated to Prof. Hartmut Herrmann, whose pioneering work and visionary approaches are an inspiration to us and have immensely advanced our understanding of aqueous-phase atmospheric chemistry. We thank Dr. Maren Pink (IUMSC) for assistance with powder X-ray diffraction measurements, Dr. Daniele Firak (TROPOS) for advice regarding the Fe^{2+} assay, Prof. Sara Skrabalak (IU) for providing access to the UV−visible spectrometer, and Drs. Markus Ammann and Natasha Garner (PSI) for helpful discussions.

■ REFERENCES

(1) Finlayson-Pitts, B. J.; Pitts, J. N. *Chemistry of the Upper and Lower Atmosphere: Theory, Experiments, and Applications*; Academic Press, 2000, p 969.

(2) Stavrakou, T.; Müller, J. F.; Boersma, K. F.; van der A, R. J.; Kurokawa, J.; Ohara, T.; Zhang, Q. Key chemical NO_x sink uncertainties and how they influence top-down emissions of nitrogen oxides. *Atmos. Chem. Phys.* **2013**, *13*, 9057−9082.

(3) Zhou, X.; Gao, H.; He, Y.; Huang, G.; Bertman, S. B.; Civerolo, K.; Schwab, J. Nitric acid photolysis on surfaces in low-NO_x environments: Significant atmospheric implications *Geophys. Res. Lett.* 2003, *30*, DOI: 10.1029/2003GL018620.

(4) Rivera-Figueroa, A. M.; Sumner, A. L.; Finlayson-Pitts, B. J. Labratory Studies of Potential Mechanisms of Renoxification of Tropospheric Nitric Acid. *Environ. Sci. Technol.* **2003**, *37*, 548−554.

(5) Baergen, A. M.; Donaldson, D. J. Photochemical renoxification of nitric acid on real urban grime. *Environ. Sci. Technol.* **2013**, *47*, 815−820.

(6) Mothes, F.; Hoffmann, E. H.; Herrmann, H. Urban Grime Photochemistry and Its Interaction with Air Pollutants NO, NO_2, and O_3: A Source for HONO and NO_2 Impacting OH in Urban Areas. *ACS Earth Space Chem.* **2023**, *7*, 2263−2274.

(7) Chatfield, R. B. Anomalous HNO_3 /NO_x ratio of remote tropospheric air: Conversion of nitric acid to formic acid and NO_x? *Geophys. Res. Lett.* **1994**, *21*, 2705−2708.

(8) Hauglustaine, D. A.; Ridley, B. A.; Solomon, S.; Hess, P. G.; Madronich, S. HNO_3/NO_x ratio in the remote troposphere During MLOPEX 2: Evidence for nitric acid reduction on carbonaceous aerosols? *Geophys. Res. Lett.* **1996**, *23*, 2609−2612.

(9) Ye, C.; Zhang, N.; Gao, H.; Zhou, X. Photolysis of Particulate Nitrate as a Source of HONO and $NO_{(x)}$. *Environ. Sci. Technol.* **2017**, *51*, 6849−6856.

(10) Reed, C.; Evans, M.; Crilley, L.; Bloss, W.; Sherwen, T.; Read, K.; Lee, J.; Carpenter, L. Evidence for renoxification in the tropical marine boundary layer. *Atmos. Chem. Phys.* **2017**, *17*, 4081−4092.

(11) Ye, C.; Heard, D. E.; Whalley, L. K. Evaluation of Novel Routes for NO_x Formation in Remote Regions. *Environ. Sci. Technol.* **2017**, *51*, 7442−7449.

(12) Zhou, X.; Civerolo, K.; Dai, H.; Huang, G.; Schwab, J.; Demerjian, K. Summertime nitrous acid chemistry in the atmospheric boundary layer at a rural site in New York State. *J. Geophys. Res.: Atmos.* **2002**, *107*, ACH 13-11.

(13) Zellner, R.; Exner, M.; Herrmann, H. Absolute OH quantum yields in the laser photolysis of nitrate, nitrite and dissolved H_2O_2 at 308 and 351 nm in the temperature range 278−353 K. *J. Atmos. Chem.* **1990**, *10*, 411−425.

(14) Benedict, K. B.; McFall, A. S.; Anastasio, C. Quantum Yield of Nitrite from the Photolysis of Aqueous Nitrate above 300 nm. *Environ. Sci. Technol.* **2017**, *51*, 4387−4395.

(15) Herrmann, H. On the photolysis of simple anions and neutral molecules as sources of O^-/OH, SO_x^- and Cl in aqueous solution. *Phys. Chem. Chem. Phys.* **2007**, *9*, 3935−3964.
(16) Ye, C.; Zhou, X.; Pu, D.; Stutz, J.; Festa, J.; Spolaor, M.; Tsai, C.; Cantrell, C.; Mauldin, R. L., 3rd; Campos, T.; Weinheimer, A.; Hornbrook, R. S.; Apel, E. C.; Guenther, A.; Kaser, L.; Yuan, B.; Karl, T.; Haggerty, J.; Hall, S.; Ullmann, K.; Smith, J. N.; Ortega, J.; Knote, C. Rapid cycling of reactive nitrogen in the marine boundary layer. *Nature* **2016**, *532*, 489−491.
(17) Romer, P. S.; Wooldridge, P. J.; Crounse, J. D.; Kim, M. J.; Wennberg, P. O.; Dibb, J. E.; Scheuer, E.; Blake, D. R.; Meinardi, S.; Brosius, A. L.; Thames, A. B.; Miller, D. O.; Brune, W. H.; Hall, S. R.; Ryerson, T. B.; Cohen, R. C. Constraints on Aerosol Nitrate Photolysis as a Potential Source of HONO and NO_x. *Environ. Sci. Technol.* **2018**, *52*, 13738−13746.
(18) Andersen, S. T.; Carpenter, L.; Reed, C.; Lee, J.; Chance, R.; Sherwen, T.; Vaughan, A.; Stewart, J.; Edwards, P.; Bloss, W.; Sommariva, R.; Crilley, L.; Nott, G.; Neves, L.; Read, K.; Heard, D.; Seakins, P.; Whalley, L.; Boustead, G.; Fleming, L.; Stone, D.; Fomba, K. Extensive Field evidence for the release of HONO from the photolysis of nitrate aerosols. *Sci. Adv.* **2023**, *9*, No. eadd6266.
(19) Shah, V.; Keller, C. A.; Knowland, K. E.; Christiansen, A.; Hu, L.; Wang, H.; Lu, X.; Alexander, B.; Jacob, D. J. Particulate Nitrate Photolysis as a Possible Driver of Rising Tropospheric Ozone. *Geophys. Res. Lett.* **2024**, *51*, No. e2023GL107980.
(20) Kasibhatla, P.; Sherwen, T.; Evans, M.; Carpenter, L.; Reed, C.; Alexander, B.; Chen, Q.; Sulprizio, M.; Lee, J.; Read, K.; Bloss, W.; Crilley, L.; Keene, W.; Pszenny, A.; Hodzic, A. Global impact of nitrate photolysis in sea-salt aerosol on NO_x, OH, and O_3 in the marine boundary layer. *Atmos. Chem. Phys.* **2018**, *18*, 11185−11203.
(21) González-Sánchez, J. M.; Huix-Rotllant, M.; Brun, N.; Morin, J.; Demelas, C.; Durand, A.; Ravier, S.; Clément, J.-L.; Monod, A. Direct formation of HONO through aqueous-phase photolysis of organic nitrates. *Atmos. Chem. Phys.* **2023**, *23*, 15135−15147.
(22) Goldstein, S.; Rabani, J. Mechanism of Nitrite Formation by Nitrate Photolysis inAqueous Solutions: The Role of Peroxynitrite, NitrogenDioxide, and Hydroxyl Radical. *J. Am. Chem. Soc.* **2007**, *129*, 10597−10601.
(23) Gen, M.; Liang, Z.; Zhang, R.; Go Mabato, B. R.; Chan, C. K. Particulate nitrate photolysis in the atmosphere. *Environ. Sci.: Atmos.* **2022**, *2*, 111−127.
(24) Romer, P. S.; Wooldridge, P. J.; Crounse, J. D.; Kim, M. J.; Wennberg, P. O.; Dibb, J. E.; Scheuer, E.; Blake, D. R.; Meinardi, S.; Brosius, A. L.; Thames, A. B.; Miller, D. O.; Brune, W. H.; Hall, S. R.; Ryerson, T. B.; Cohen, R. C. Constraints on Aerosol Nitrate Photolysis as a Potential Source of HONO and $NO_{(x)}$. *Environ. Sci. Technol.* **2018**, *52*, 13738−13746.
(25) Shi, Q.; Tao, Y.; Krechmer, J. E.; Heald, C. L.; Murphy, J. G.; Kroll, J. H.; Ye, Q. Laboratory Investigation of Renoxification from the Photolysis of Inorganic Particulate Nitrate. *Environ. Sci. Technol.* **2021**, *55*, 854−861.
(26) Ye, C.; Gao, H.; Zhang, N.; Zhou, X. Photolysis of Nitric Acid and Nitrate on Natural and Artificial Surfaces. *Environ. Sci. Technol.* **2016**, *50*, 3530−3536.
(27) Nanayakkara, C. E.; Jayaweera, P. M.; Rubasinghege, G.; Baltrusaitis, J.; Grassian, V. H. Surface photochemistry of adsorbed nitrate: the role of adsorbed water in the formation of reduced nitrogen species on alpha-Fe_2O_3 particle surfaces. *J. Phys. Chem. A* **2014**, *118*, 158−166.
(28) Nissenson, P.; Dabdub, D.; Das, R.; Maurino, V.; Minero, C.; Vione, D. Evidence of the water-cage effect on the photolysis of NO_3^- and $FeOH_2^+$. Implications of this effect and of H_2O_2 surface accumulation on photochemistry at the air−water interface of atmospheric droplets. *Atmos. Environ.* **2010**, *44*, 4859−4866.
(29) Nissenson, P.; Knox, C. J.; Finlayson-Pitts, B. J.; Phillips, L. F.; Dabdub, D. Enhanced photolysis in aerosols: evidence for important surface effects. *Phys. Chem. Chem. Phys.* **2006**, *8*, 4700−4710.
(30) Wingen, L. M.; Moskun, A. C.; Johnson, S. N.; Thomas, J. L.; Roeselova, M.; Tobias, D. J.; Kleinman, M. T.; Finlayson-Pitts, B. J. Enhanced surface photochemistry in chloride-nitrate ion mixtures. *Phys. Chem. Chem. Phys.* **2008**, *10*, 5668−5677.
(31) Wang, Y.; Huang, D. D.; Huang, W.; Liu, B.; Chen, Q.; Huang, R.; Gen, M.; Mabato, B. R. G.; Chan, C. K.; Li, X.; Hao, T.; Tan, Y.; Hoi, K. I.; Mok, K. M.; Li, Y. J. Enhanced Nitrite Production from the Aqueous Photolysis of Nitrate in the Presence of Vanillic Acid and Implications for the Roles of Light-Absorbing Organics. *Environ. Sci. Technol.* **2021**, *55*, 15694−15704.
(32) Ye, C.; Zhang, N.; Gao, H.; Zhou, X. Matrix effect on surface-catalyzed photolysis of nitric acid. *Sci. Rep.* **2019**, *9*, No. 4351.
(33) Handley, S. R.; Clifford, D.; Donaldson, D. Photochemical loss of nitric acid on organic films: a possible recycling mechanism for NO_x. *Environ. Sci. Technol.* **2007**, *41*, 3898−3903.
(34) Wang, X.; Dalton, E. Z.; Payne, Z. C.; Perrier, S.; Riva, M.; Raff, J. D.; George, C. Superoxide and Nitrous Acid Production from Nitrate Photolysis Is Enhanced by Dissolved Aliphatic Organic Matter. *Environ. Sci. Technol. Lett.* **2021**, *8*, 53−58.
(35) West, C. P.; Morales, A. C.; Ryan, J.; Misovich, M. V.; Hettiyadura, A. P. S.; Rivera-Adorno, F.; Tomlin, J. M.; Darmody, A.; Linn, B. N.; Lin, P.; Laskin, A. Molecular investigation of the multi-phase photochemistry of Fe(III)-citrate in aqueous solution. *Environ. Sci.: Processes Impacts* **2022**, 190−213.
(36) Li, Q.; Ma, S.; Liu, Y.; Wu, X.; Fu, H.; Tu, X.; Yan, S.; Zhang, L.; George, C.; Chen, J. Phase State Regulates Photochemical HONO Production from $NaNO_3$/Dicarboxylic Acid Mixtures. *Environ. Sci. Technol.* **2024**, *58*, 7516−7528.
(37) García, S. L. M.; Gutierrez, I.; Nguyen, J. V.; Navea, J. G.; Grassian, V. H. Enhanced HONO Formation from Aqueous Nitrate Photochemistry in the Presence of Marine Relevant Organics: Impact of Marine-Dissolved Organic Matter (m-DOM) Concentration on HONO Yields and Potential Synergistic Effects of Compounds within m-DOM. *ACS ES&T Air* **2024**, *1*, 525−535.
(38) Wang, S.; Ackermann, R.; Spicer, C. W. et al. Atmospheric observations of enhanced NO_2-HONO conversion on mineral dust particles *Geophys. Res. Lett.* 2003, *30*, DOI: 10.1029/2003gl017014.
(39) Cwiertny, D. M.; Young, M. A.; Grassian, V. H. Chemistry and photochemistry of mineral dust aerosol. *Annu. Rev. Phys. Chem.* **2008**, *59*, 27−51.
(40) Kebede, M. A.; Bish, D. L.; Losovyj, Y.; Engelhard, M. H.; Raff, J. D. The Role of Iron-Bearing Minerals in NO_2 to HONO Conversion on Soil Surfaces. *Environ. Sci. Technol.* **2016**, *50*, 8649−8660.
(41) Scharko, N. K.; Martin, E. T.; Losovyj, Y.; Peters, D. G.; Raff, J. D. Evidence for Quinone Redox Chemistry Mediating Daytime and Nighttime NO_2-to-HONO Conversion on Soil Surfaces. *Environ. Sci. Technol.* **2017**, *51*, 9633−9643.
(42) Chen, H.; Laskin, A.; Baltrusaitis, J.; Gorski, C. A.; Scherer, M. M.; Grassian, V. H. Coal fly ash as a source of iron in atmospheric dust. *Environ. Sci. Technol.* **2012**, *46*, 2112−2120.
(43) Chen, H.; Grassian, V. H. Iron dissolution of dust source materials during simulated acidic processing: the effect of sulfuric, acetic, and oxalic acids. *Environ. Sci. Technol.* **2013**, *47*, 10312−10321.
(44) Weller, C.; Tilgner, A.; Brauer, P.; Herrmann, H. Modeling the impact of iron-carboxylate photochemistry on radical budget and carboxylate degradation in cloud droplets and particles. *Environ. Sci. Technol.* **2014**, *48*, 5652−5659.
(45) Zepp, R. G. Hydroxyl Radical Formation in Aqueous Reactions (pH 3−8) of Iron(II) with Hydrogen Peroxide: The Photo-Fenton Reaction. *Environ. Sci. Technol.* **1992**, *25*, 313−319.
(46) Vermilyea, A. W.; Voelker, B. Photo-Fenton Reaction at Near Neutral pH. *Environ. Sci. Technol.* **2009**, *43*, 6927−6933.
(47) Stumm, W.; M, J. J. *Aquatic Chemistry*, 3rd ed.; Wiley & Sons, Inc., 1996.
(48) Donaldson, M. A.; Bish, D. L.; Raff, J. D. Soil surface acidity plays a determining role in the atmospheric-terrestrial exchange of nitrous acid. *Proc. Natl. Acad. Sci. U.S.A.* **2014**, *111*, 18472−18477.
(49) Payne, Z. C.; Dalton, E. Z.; Gandolfo, A.; Raff, J. D. HONO Measurement by Catalytic Conversion to NO on Nafion Surfaces. *Environ. Sci. Technol.* **2023**, *57*, 85−95.

(50) Su, H.; Cheng, Y.; Oswald, R.; Behrendt, T.; Trebs, I.; Meixner, F. X.; Andreae, M. O.; Cheng, P.; Zhang, Y.; Pöschl, U. Soil Nitrite as a Source of Atmospheric HONO and OH Radicals. *Science* **2011**, *333*, 1616−1618.
(51) Daugherty, E. E.; Gilbert, B.; Nico, P. S.; Borch, T. Complexation and Redox Buffering of Iron(II) by Dissolved Organic Matter. *Environ. Sci. Technol.* **2017**, *51*, 11096−11104.
(52) International Humic Substances Society 2023.
(53) Cwiertny, D. M.; Baltrusaitis, J.; Hunter, G. J.; Laskin, A.; Scherer, M. M.; Grassian, V. H. Characterization and acid-mobilization study of iron-containing mineral dust source materials *J. Geophys. Res.: Atmos* 2008, *113*, DOI: 10.1016/j.atmos-env.2004.07.010.
(54) Krueger, B. J.; Grassian, V. H.; Cowin, J. P.; Laskin, A. Heterogeneous chemistry of individual mineral dust particles from different dust source regions: the importance of particle mineralogy. *Atmos. Environ.* **2004**, *38*, 6253−6261.
(55) Lueder, U.; Jorgensen, B. B.; Maisch, M.; Schmidt, C.; Kappler, A. Influence of Fe(III) source, light quality, photon flux and presence of oxygen on photoreduction of Fe(III)-organic complexes - Implications for light-influenced coastal freshwater and marine sediments. *Sci. Total Environ.* **2022**, *814*, No. 152767.
(56) Waite, T. D.; Morel, F. M. M. Photoreductive Dissolution of Colloidal Iron Oxides in Natural Waters. *Environ. Sci. Technol.* **1984**, *18*, 860−868.
(57) Borer, P.; Sulzberger, B.; Hug, S. J.; Kraemer, S. M.; Kretzschmar, R. Photoreductive dissolution of iron(III) (hydr)oxides in the absence and presence of organic ligands: experimental studies and kinetic modeling. *Environ. Sci. Technol.* **2009**, *43*, 1864−1870.
(58) Weller, C.; Horn, S.; Herrmann, H. Photolysis of Fe(III) carboxylato complexes: Fe(II) quantum yields and reaction mechanisms. *J. Photochem. Photobiol., A* **2013**, *268*, 24−36.
(59) Zhang, Y.; Richards, D. S.; Grotemeyer, E. N.; Jackson, T. A.; Schöneich, C. Near-UV and Visible Light Degradation of Iron (III)-Containing Citrate Buffer: Formation of Carbon Dioxide Radical Anion via Fragmentation of a Sterically Hindered Alkoxyl Radical. *Mol. Pharmaceutics* **2022**, *19*, 4026−4042.
(60) Garg, S.; Jiang, C.; Miller, C. J.; Rose, A. L.; Waite, T. D. Iron Redox Transformations in Continuously Photolyzed Acidic Solutions Containing Natural Organic Matter: Kinetic and Mechanistic Insights. *Environ. Sci. Technol.* **2013**, *47*, 9190−9197.
(61) Wieland, E.; Stumm, W. Dissolution kinetics of kaolinite in acidic aqueous solutions at 25°C. *Geochim. Cosmochim. Acta* **1992**, *56*, 3339−3355.
(62) Zhu, C.; Jagdale, G.; Gandolfo, A.; Alanis, K.; Abney, R.; Zhou, L.; Bish, D.; Raff, J.; Baker, L. Surface Charge Measurements with Scanning Ion Conductance Microscopy Provide Insights into Nitrous Acid Speciation at the Kaolin Mineral-Air Interface. *Environ. Sci. Technol.* **2021**, *55*, 12233−12242.
(63) Alpert, P. A.; Dou, J.; Corral Arroyo, P.; Schneider, F.; Xto, J.; Luo, B.; Peter, T.; Huthwelker, T.; Borca, C. N.; Henzler, K. D.; Schaefer, T.; Herrmann, H.; Raabe, J.; Watts, B.; Krieger, U. K.; Ammann, M. Photolytic radical persistence due to anoxia in viscous aerosol particles. *Nat. Commun.* **2021**, *12*, No. 1769.
(64) Cwiertny, D. M.; Hunter, G. J.; Pettibone, J. M.; Scherer, M. M.; Grassian, V. H. Surface Chemistry and Dissolution of alpha-FeOOH Nanorods and Microrods: Environmental Implications of Size-Dependent Interactions with Oxalate. *J. Phys. Chem. C* **2009**, *113*, 2175−2186.
(65) Rubasinghege, G.; Grassian, V. H. Photochemistry of Adsorbed Nitrate on Aluminum Oxide Particle Surfaces. *J. Phys. Chem. A* **2009**, *113*, 7818−7825.
(66) Homyak, P. M.; Kamiyama, M.; Sickman, J. O.; Schimel, J. P. Acidity and organic matter promote abiotic nitric oxide production in drying soils. *Global Change Biol.* **2017**, *23*, 1735−1747.
(67) Burgess, D. R. *NIST SRD 46. Critically Selected Stability Constants of Metal Complexes: Version 8.0 for Windows*; National Institute of Standards and Technology, 2004. (acccessed on October 24, 2024).
(68) Dubowski, Y.; Colussi, A. J.; Boxe, C.; Hoffmann, M. R. monotonic-increase of nitrite yields in the photolysis of nitrate in ice and water between 238 and 294K. *J. Phys. Chem. A* **2002**, *106*, 6967−6971.
(69) Scharko, N. K.; Berke, A. E.; Raff, J. D. Release of nitrous acid and nitrogen dioxide from nitrate photolysis in acidic aqueous solutions. *Environ. Sci. Technol.* **2014**, *48*, 11991−12001.
(70) Stemmler, K.; Ammann, M.; Donders, C.; Kleffmann, J.; George, C. Photosensitized reduction of nitrogen dioxide on humic acid as a source of nitrous acid. *Nature* **2006**, *440*, 195−198.
(71) Grätzel, M.; Henglein, A.; Taniguchi, S. Pulsradiolytische Beobachtungen über die Reduktion des NO_3^--Ions und über Bildung und Zerfall der persalpetrigen Säure in wäßriger Lösung. *Ber. Bunsenges. Phys. Chem.* **1970**, *74*, 292−298.
(72) Jaccard, C. Paramagnetic Nitrogen Oxides in Irradiated Potassium Halides. *Phys. Rev.* **1961**, *124*, No. 60.
(73) Cook, A. R.; Dimitrijevic, N.; Dreyfus, B.; Meisel, D.; Curtiss, L.; Camaioni, D. Reducing Radicals in Nitrate Solutions. The NO_3^{2-} System Revisited. *J. Phys. Chem. A* **2001**, *105*, 3658−3666.
(74) Kim, P.; Boothby, C.; Grassian, V. H.; Continetti, R. E. Photoinduced Reactions of Nitrate in Aqueous Microdroplets by Triplet Energy Transfer. *J. Phys. Chem. Lett.* **2023**, *14*, 10677−10684.
(75) Cottrell, B. A.; Gonsior, M.; Timko, S. A.; Simpson, A. J.; Cooper, W. J.; van der Veer, W. Photochemistry of marine and fresh waters: A role for copper−dissolved organic matter ligands. *Mar. Chem.* **2014**, *162*, 77−88.
(76) Semitsoglou-Tsiapou, S.; Mous, A.; Templeton, M. R.; Graham, N. J. D.; Leal, L. H.; Kruithof, J. C. The role of natural organic matter in nitrite formation by LP-UV/H_2O_2 treatment of nitrate-rich water. *Water Res.* **2016**, *106*, 312−319.
(77) Cottrell, B. A.; Timko, S. A.; Devera, L.; Robinson, A. K.; Gonsior, M.; Vizenor, A. E.; Simpson, A. J.; Cooper, W. J. Photochemistry of excited-state species in natural waters: a role for particulate organic matter. *Water Res.* **2013**, *47*, 5189−5199.
(78) Sumner, A. L.; Menke, E. J.; Dubowski, Y.; Newberg, J. T.; Penner, R. M.; Hemminger, J. C.; Wingen, L. M.; Brauers, T.; Finlayson-Pitts, B. J. The nature of water on surfaces of laboratory systems and implications for heterogeneous chemistry in the troposphere. *Phys. Chem. Chem. Phys.* **2004**, *6*, 604−613.
(79) Rubasinghege, G.; Grassian, V. H. Role(s) of adsorbed water in the surface chemistry of environmental interfaces. *Chem. Commun.* **2013**, *49*, 3071−3094.
(80) Janik, I.; Tripathi, G. N. The nature of the CO2$^-$ radical anion in water. *J. Chem. Phys.* **2016**, *144*, No. 154307.
(81) Chen, G.; Hanukovich, S.; Chebeir, M.; Christopher, P.; Liu, H. Nitrate Removal via a Formate Radical-Induced Photochemical Process. *Environ. Sci. Technol.* **2019**, *53*, 316−324.
(82) Dou, J.; Alpert, P. A.; Corral Arroyo, P.; Luo, B.; Schneider, F.; Xto, J.; Huthwelker, T.; Borca, C. N.; Henzler, K. D.; Raabe, J.; Watts, B.; Herrmann, H.; Peter, T.; Ammann, M.; Krieger, U. K. Photochemical degradation of iron(III) citrate/citric acid aerosol quantified with the combination of three complementary experimental techniques and a kinetic process model. *Atmos. Chem. Phys.* **2021**, *21*, 315−338.
(83) Zhang, Y.; Richards, D. S.; Grotemeyer, E. N.; Jackson, T. A.; Schoneich, C. Near-UV and Visible Light Degradation of Iron (III)-Containing Citrate Buffer: Formation of Carbon Dioxide Radical Anion via Fragmentation of a Sterically Hindered Alkoxyl Radical. *Mol. Pharmaceutics* **2022**, *19*, 4026−4042.
(84) Chena, J.; Jianyong, L.; Zhoua, J.; Chenb, D. Reductive removal of nitrate by carbon dioxide radical with high product selectivity to form N_2 in a UV/H_2O_2/HCOOH system. *J. Water Process Eng.* **2020**, *33*, No. 101097.
(85) Miller, W. L.; Zepp, R. G. Photochemical production of dissolved inorganic carbon from terrestrial organic matter: Significance to the oceanic organic carbon cycle. *Geophys. Res. Lett.* **1995**, *22*, 417−420.
(86) Kieber, R. J.; Zhou, X.; Mopper, K. Formation of carbonyl compounds from UV-induced photodegradation of humic substances

in natural waters: Fate of riverine carbon in the sea. *Limnol. Oceanogr.* **2003**, *35*, 1503−1515.
(87) Nowak, S.; Lafon, S.; Caquineau, S.; Journet, E.; Laurent, B. Quantitative study of the mineralogical composition of mineral dust aerosols by X-ray diffraction. *Talanta* **2018**, *186*, 133−139.
(88) Zhu, X.; Prospero, J. M.; Millero, F. J.; Savoie, D. L.; Brass, G. W. The solubility of ferric ion in marine mineral aerosol solutions at ambient relative humidities. *Mar. Chem.* **1992**, *38*, 91−107.
(89) Meskhidze, N.; Chameides, W. L.; Nenes, A.; Chen, G. Iron mobilization in mineral dust: Can anthropogenic SO_2 emissions affect ocean productivity? *Geophys. Res. Lett.* **2003**, *30*, No. 2085.
(90) Li, Z.; Yim, S. H.-L.; Ho, K.-F. High temporal resolution prediction of street-level PM2.5 and NO_x concentrations using machine learning approach. *J. Cleaner Prod.* **2020**, *268*, No. 121975.
(91) Bloss, W. J.; Kramer, L.; Crilley, L. R.; Vu, T.; Harrison, R. M.; Shi, Z.; Lee, J. D.; Squires, F. A.; Whalley, L. K.; Slater, E.; Woodward-Massey, R.; Ye, C.; Heard, D. E.; Tong, S.; Hou, S.; Sun, Y.; Xu, J.; Wei, L.; Fu, P. Insights into air pollution chemistry and sulphate formation from nitrous acid (HONO) measurements during haze events in Beijing. *Faraday Discuss.* **2021**, *226*, 223−238.
(92) Jiang, Y.; Hoffmann, E. H.; Tilgner, A.; Aiyuk, M. B. E.; Andersen, S. T.; Wen, L.; van Pinxteren, M.; Shen, H.; Xue, L.; Wang, W.; Herrmann, H. Insights Into NO and HONO Chemistry in the Tropical Marine Boundary Layer at Cape Verde During the MarParCloud Campaign. *J. Geophys. Res.: Atmos.* **2023**, *128*, No. e2023JD038865.
(93) Kleffmann, J. Daytime sources of nitrous acid (HONO) in the atmospheric boundary layer. *ChemPhysChem* **2007**, *8*, 1137−1144.
(94) Lee, J. D.; Whalley, L. K.; Heard, D. E.; Stone, D.; Dunmore, R. E.; Hamilton, J. F.; Young, D. E.; Allan, J. D.; Laufs, S.; Kleffmann, J. Detailed budget analysis of HONO in central London reveals a missing daytime source. *Atmos. Chem. Phys.* **2016**, *16*, 2747−2764.

https://doi.org/10.1021/acsearthspacechem.4c00252
ACS Earth Space Chem. 2024, 8, 2587−2598